RESEARCH ARTICLE

THE FASEB JOURNAL

CHARGE syndrome-associated proteins FAM172A and CHD7 influence male sex determination and differentiation through transcriptional and alternative splicing mechanisms

Catherine Bélanger[1,2] | Tatiana Cardinal[1,2] | Elizabeth Leduc[1,2] | Robert S. Viger[3,4] | Nicolas Pilon[1,2,5]

[1]Molecular Genetics of Development Laboratory, Département des Sciences Biologiques, Université du Québec à Montréal (UQAM), Montréal, Québec, Canada

[2]Centre d'Excellence en Recherche sur les Maladies Orphelines – Fondation Courtois (CERMO-FC), Université du Québec à Montréal, Montréal, Québec, Canada

[3]Reproduction, Mother and Child Health, Centre de recherche en reproduction, développement et santé intergénérationnelle (CRDSI), Centre de recherche du CHU de Québec-Université Laval, Quebec City, Québec, Canada

[4]Department of Obstetrics, Gynecology, and Reproduction, Faculty of Medicine, Université Laval, Quebec City, Québec, Canada

[5]Département de pédiatrie, Université de Montréal, Montréal, Québec, Canada

Correspondence
Nicolas Pilon, Département des Sciences Biologiques, and Centre d'excellence en recherche sur les maladies orphelines – Fondation Courtois, Université du Québec à Montréal, 141 Avenue du Président-Kennedy, Montréal H2X 3Y7, Québec, Canada.
Email: pilon.nicolas@uqam.ca

Present address
Catherine Bélanger, Biopterre - Bureau biotechnologie et laboratoire, 1642 rue de la Ferme, La Pocatière, Québec G0R 1Z0, Canada

Abstract

To gain further insight into chromatin-mediated regulation of mammalian sex determination, we analyzed the role of the CHARGE syndrome-associated proteins FAM172A and CHD7. This study is based on our prior discoveries that a subset of corresponding mutant mice display complete male-to-female sex reversal, and that both of these proteins regulate co-transcriptional alternative splicing in neural crest cells. Here, we report that FAM172A and CHD7 are present in the developing gonads when sex determination normally occurs in mice. The interactome of FAM172A in pre-Sertoli cells again suggests a role at the chromatin-spliceosome interface, like in neural crest cells. Accordingly, analysis of *Fam172a*-mutant pre-Sertoli cells revealed transcriptional and splicing dysregulation of hundreds of genes. Many of these genes are similarly affected in *Chd7*-mutant pre-Sertoli cells, including several known key regulators of sex determination and subsequent formation of testis cords. Among them, we notably

---

Abbreviations: ANOVA, analysis of variance; CHARGE, coloboma of the eye, heart defects, atresia of choanae, retardation of growth/development, genital abnormalities, and ear anomalies; ChIP, chromatin immunoprecipitation; DAPI, 4′,6-Diamidino-2-Phenylindole; DMEM, Dulbecco's modified eagle medium; EDTA, Ethylenediaminetetraacetic acid; EGTA, ethyleneglycoltetraacetic acid; EMEM, Eagle's minimum essential medium; FACS, fluorescence-activated cell sorting; GO, gene ontology; LC-MS/MS, liquid chromatography with tandem mass spectrometry; MBP, maltose-binding protein; PBS, phosphate-buffered saline; PCR, polymerase chain reaction; PFA, paraformaldehyde; PGR9E11, porcine genital ridge clone 9E11; qPCR, quantitative polymerase chain reaction; RFP, red fluorescent protein; RNA-seq, RNA sequencing; SDS, sodium dodecyl sulfate; SEM, standard error of the mean; TCA, trichloroacetic acid; TS, tail somite.

---

identified *Sry* as a direct transcriptional target and WNT pathway-associated *Lef1* and *Tcf7l2* as direct splicing targets. The identified molecular defects are also associated with the abnormal morphology of seminiferous tubules in mutant postnatal testes. Altogether, our results thus identify FAM172A and CHD7 as new players in the regulation of male sex determination and differentiation in mice, and further highlight the importance of chromatin-mediated regulatory mechanisms in these processes.

KEYWORDS

alternative splicing, CHARGE syndrome, CHD7, FAM172A, Sex reversal, transcription

1 | INTRODUCTION

The study of mammalian sex determination has seen considerable breakthroughs in the last decade. Since the discovery of the HMG-box transcription factor SRY (Sex-determining region Y) as the first molecular switch controlling the bipotential gonad toward a testicular or ovarian fate, our understanding of the mechanisms of mammalian sex determination has evolved to include several factors (sometimes opposing one another) acting at different steps in the gene expression process.[1,2] Among them, chromatin regulators and epigenetic factors now appear to play central roles in fine-tuning the expression of key sex-determining genes.[3,4] A notable example is histone demethylase JMJD1A, which was identified as a critical factor for removing H3K9me3 repressive marks at the *Sry* locus, thereby enabling proper *Sry* spatiotemporal expression in murine pre-Sertoli cells at the time of sex determination (around embryonic day (e) 11.5).[5,6] Consistent with this key role, lack of JMJD1A function in mice leads to complete, highly penetrant male-to-female sex reversal.[5]

Alternative splicing is now also recognized as a key regulatory mechanism of sex determination and differentiation. This role has been notably well described in insects, fish, and reptiles,[7–11] and recent findings support a similar role in mammals. Indeed, RNA-seq experiments in mice revealed the existence of hundreds of differentially expressed transcript isoforms in male and female gonads around the time of sex determination and early sex differentiation.[12,13] Well-known examples include *Wt1* and *Fgfr2* genes, which both code for at least two major alternatively spliced isoforms. WT1 protein isoforms differ by the inclusion (+KTS) or exclusion (−KTS) of a short peptide motif that is required for upregulating *Sry* transcription.[14] FGFR2 isoforms differ in the composition of the C-terminal half of the third Ig-like loop in the FGF binding domain (generating isoforms IIIb and IIIc), with isoform IIIc being critically required for mediating male-determining FGF9 signaling in pre-Sertoli cells.[15,16] Long since considered to be a single exon gene, even *Sry* is now known to be

alternatively spliced to include or not a second exon that confers greater stability and sex-determining activity to the SRY protein.[17] Another intriguing alternatively spliced gene is *Lef1* (Lymphoid Enhancer Binding Factor 1), for which transcripts containing the alternative exon 6 were found to be enriched in female gonads during early sex differentiation.[13] Inclusion of this alternative exon is necessary for full activity of the LEF1 protein as a transcriptional effector of canonical WNT signaling[18]—a critical signaling pathway for ovarian development[19] also necessary for proper differentiation of Sertoli cells in males.[20] All these observations are thus consistent with an important role for alternative splicing in mammalian sex determination/differentiation, but the manner by which identified splicing events are regulated remains largely unexplored besides a single study reporting an important role for SOX9.[21]

We previously showed that dysregulation of co-transcriptional alternative splicing constitutes a common disease mechanism for genetically distinct cases of *coloboma of the eye, heart defects, atresia of choanae, retardation of growth/development, genital abnormalities, and ear anomalies* (CHARGE) syndrome—a rare multi-organ malformation condition mainly affecting neural crest-derived tissues.[22] This previous work allowed us to propose a model whereby the co-transcriptional regulator FAM172A (Family with sequence similarity 172, member A), the chromatin remodeler CHD7 (Chromodomain helicase DNA-binding protein 7), and the small RNA binding protein AGO2 (Argonaute 2) appear to coordinately stabilize the interface between chromatin and spliceosome machineries at alternatively spliced exons in neural crest cells, most likely without direct binding to DNA or mRNA.[23] Yet, we and others have shown that these proteins can also influence gene expression levels independently of alternative splicing.[22,24,25] Unexpectedly, our prior work further revealed the presence of a partially penetrant male-to-female sex reversal phenotype in both homozygous *Fam172a*$^{Tp/Tp}$ [*Toupee*] (affecting 25% of XY animals) and heterozygous *Chd7*$^{Gt/+}$ (affecting 12% of XY animals) mouse models of CHARGE syndrome.[22]

Moreover, a higher incidence of sex reversal was noted in $Fam172a^{Tp/+}$;$Chd7^{Gt/+}$ double heterozygous mutants (affecting 33% of XY animals).[22] These observations thus suggest that transcription and alternative splicing regulation are dual roles shared by FAM172A and CHD7 in the context of sex determination as well, at least in mice.

In the current study, we specifically examined the role of FAM172A and CHD7 in the control of male sex determination. We discovered that the partial loss of either $Fam172a$ or $Chd7$ leads to extensive dysregulation of transcription and alternative splicing in pre-Sertoli cells, including direct impacts on transcription of the male determining gene Sry and alternative splicing of the WNT effector genes $Lef1$ and $Tcf7l2$. Globally, our results thus suggest that FAM172A and CHD7 are equally important regulators of mouse sex determination and Sertoli cell differentiation at both the transcriptional and alternative splicing levels.

2 | MATERIALS AND METHODS

2.1 | Mice

Animal experimental protocols were approved by the institutional ethics committee of the University of Quebec at Montreal (*Comité institutionnel de protection des animaux* [CIPA]; Reference number: 650). Details about the generation of $Fam172a^{Tp/Tp}$ (*Toupee*; FVB/N background), $Chd7^{Gt/+}$ (129 Sv-C57BL/6J mixed background; kindly provided by Dr. Donna M. Martin from University of Michigan Medical School) and $Gata4p[5kb]$-RFP transgenic mouse lines can be found elsewhere.[22,26–28] All lines were maintained in the FVB/N genetic background, after five rounds of successive backcross with wild-type FVB/N mice in the case of $Chd7^{Gt/+}$. For high-throughput transcriptome sequencing, $Fam172a^{Tp}$ and $Chd7^{Gt}$ alleles were introduced in the $Gata4p[5kb]$-RFP transgenic background by breeding, with single $Gata4p[5kb]$-RFP transgenic mice used as controls. PCR-based chromosomal sexing and genotyping of $Fam172a^{Tp}$ and $Chd7^{Gt}$ alleles were performed as previously described,[22] using primers listed in Table S1. Embryos were generated by natural mating and collected at e11.5 or e12.5, with noon of the day of vaginal plug detection designated as e0.5. Embryos were carefully staged by counting the number of tail somites and sexed using either morphological criteria (presence of cords and coelomic vessel in e12.5 testis) or PCR as mentioned above.

2.2 | Tissue labeling and imaging

In situ hybridization of Sry,[27] hematoxylin-eosin staining of paraffin-embedded testes,[29] and immunolabeling of gonadal cells[22] or cryosections[30] were performed as previously described. For whole-mount immunofluorescence staining, gonads from e11.5 and e12.5 embryos were dissected in ice-cold PBS, fixed in 4% PFA overnight at 4°C, and gradually dehydrated into methanol for storage at −20°C. For staining per se, gonads were gradually rehydrated in PBS, permeabilized in PBS containing 0.1% TritonX-100 for 1 h, and transferred into blocking solution (PBS 1% TritonX-100, 10% fetal bovine serum) for 1 h at room temperature. Gonads were then incubated in relevant primary and secondary antibodies diluted in blocking solution overnight at 4°C, with three 30-min washes in between (using 0.1% TritonX-100). Gonads were finally counterstained with DAPI (5 µg/ml in 0.1% TritonX-100) for 5 min, extensively washed (3 × 30 min, in 0.1% TritonX-100 once and PBS twice), and finally transferred to 80% glycerol at 4°C until imaging. Primary antibodies used were rabbit anti-FAM172A (Abcam #ab121364; diluted 1:250), rabbit anti-CHD7 (Cell Signaling #6505; diluted 1:250), mouse anti-GATA4 (Santa-Cruz #sc-25310; diluted 1:250), rabbit anti-COL4 (Abcam #ab6586; diluted 1:400) and rabbit anti-ITGA6 (Abcam #ab181551; diluted 1:400). Corresponding secondary antibodies were donkey Alexa Fluor 594 anti-rabbit IgG (Jackson Immunoresearch #711-585–152; diluted 1:500), donkey Alexa Fluor 647 anti-mouse IgG (Jackson Immunoresearch #715-605–150; diluted 1:500) or donkey Alexa Fluor 647 anti-rabbit IgG (Jackson Immunoresearch #715-605–152; diluted 1:500). Images were acquired using either a 20X (Plan Fluor 20x/0.75 Mimm) or a 60X (Plan Apo VC 60x1.40 oil) objective on a Nikon A1R confocal microscope (for immunofluorescence), with a Leica M205FA stereomicroscope (for in situ hybridization), or with a Leica DM2000 upright microscope (for histology sections).

2.3 | Tissue preparation for gene expression analyses

For RT-qPCR analysis, gonads and attached mesonephroi were dissected from e11.5 embryos generated by $Fam172a^{Tp/+}$ or $Chd7^{Gt/+}$ intercrosses, and then immediately frozen at −80°C until RNA extraction. For high-throughput transcriptome analysis, gonads (with mesonephroi removed) were dissected from e12.5 embryos obtained from $Gata4p[5kb]$-RFP, $Fam172a^{Tp/Tp}$;$Gata4p[5kb]$-RFP or $Chd7^{Gt/+}$; $Gata4p[5kb]$-RFP intercrosses, and then immediately processed for FACS-mediated recovery of RFP-positive cells using previously described methods.[31] Gonad pairs were dissociated at 37°C with 1.3 mg/ml dispase II, 0.4 mg/ml collagenase, and 0.1 mg/ml DNAse I in EMEM medium for 45 min. For each pair of gonads,

between 5000 and 55 000 RFP-positive cells were collected using a BD FACSJazz cell sorter (BD Biosciences) and stored at −80°C until RNA extraction. Between 270 000 and 330 000 cells were pooled for each biological replicate and genotype. For both whole gonads and FACS-recovered cells, RNA extraction was performed using the RNeasy Plus Purification Kit (Qiagen) following the manufacturer's instructions.

2.4 | Gene expression analyses

For *Sry* expression analysis at e11.5, RT-qPCR was performed as previously described[32] using relevant primers listed in Table S1. Expression levels were normalized to the housekeeping gene *Psmb2* and non-specific background expression in XX gonads. For high-throughput transcriptome analysis at e12.5, preparation of ribosomal RNA-depleted libraries (using 100 ng of total RNA per sample as starting material) and sequencing (Illumina HiSeq 4000) were performed at Genome Quebec Innovation Center. Paired-end sequences of 100-bp in length (between 32 and 43 million reads for *Gata4p[5kb]-RFP* libraries, 37–42 million reads for *Fam172a$^{Tp/Tp}$;Gata4p[5kb]-RFP* libraries, and 53–62 million reads for *Chd7$^{Gt/+}$;Gata4p[5kb]-RFP* libraries) were mapped onto the GRCm38 reference genome. Three libraries were sequenced per genotype but one *Fam172a$^{Tp/Tp}$;Gata4p[5kb]-RFP* library was not of sufficient quality for bioinformatic analysis, which was performed at the Institut de recherches cliniques de Montreal using DESeq and rMATS (Junction counts only) pipelines. Subsequent GO analysis was performed using the WEB-based GEne SeT AnaLysis Toolkit (WebGestalt; http://www.webgestalt.org/).[33]

2.5 | Cell culture

The porcine genital ridge cell line PGR9E11 was as previously described.[34] Cells were maintained in DMEM (Wisent) supplemented with 20% calf bovine serum and penicillin/streptomycin under standard conditions (37°C and 5% CO_2). Cells were harvested between passages 15 and 25 for mass spectrometry, immunofluorescence, and ChIP-qPCR experiments.

2.6 | Affinity purification coupled to tandem mass spectrometry

PGR9E11 cell extracts (1.5 mg of proteins per sample) were passed on an amylose resin column containing immobilized $_{MBP}$FAM172A or MBP-tag alone.[22] Following extensive washing, interacting proteins were co-eluted with $_{MBP}$FAM172A or MBP-tag with column buffer (20 mM Tris-HCl pH7.4, 200 mM NaCl, 1 mM EDTA, 1X Roche Complete protease inhibitors) supplemented with 100 mM maltose. Eluates were then individually precipitated using 72% TCA, 0.3% Na-deoxycholate, and 10X Tris-EDTA (60 µg of proteins per sample). Samples were then air-dried and sent to the Proteomics Discovery platform of the Institut de Recherches Cliniques de Montreal where preparation of trypsic fragments, LC-MS/MS analysis on a LTQ Orbitrap Fusion Tribrid mass spectrometer (ThermoFisher Scientific), and peptide identification was performed. Peptides were identified using the Mascot 2.1.0.81 search engine (Matrix Science) and the UniProt_Mammals database. Results were analyzed using the Scaffold 4 software (Proteome Software version 4.8.4). Proteins identified via at least one peptide (with probability greater than 90%) were accepted as $_{MBP}$FAM172A interactors if they were enriched at least 1.5-fold in comparison to the MBP negative control and detected in at least two out of the three tested biological replicates.

2.7 | Chromatin immunoprecipitation

ChIP-qPCR was performed essentially as previously described,[22] using one confluent 100-mm plate of PGR9E11 cells per biological replicate. Briefly, cell pellets were cross-linked using 1% PFA and sonicated in nuclear lysis buffer (50 mM Tris-HCl pH 8.0, 10 mM EDTA, 1% SDS, 0,5 mM EGTA, 1X Roche Complete protease inhibitors) with sonicaQ125 using 3 rounds of 5 min cycles (15 s ON/45 s OFF) at 40% amplitude. Immunoprecipitations were performed using Protein G Dynabeads (ThermoFisher scientific) and magnetic support. For each experimental condition, 2 µg of antibodies were used (rabbit anti-FAM172A Abcam #ab121364; rabbit anti-CHD7 Cell Signaling #6505). Quantitative PCR (qPCR) was performed using the Ssofast EvaGreen Supermix and C1000 touch thermal cycler (BioRad) in accordance with the manufacturer's protocol. Primers for ChIP-qPCR are detailed in Table S1.

2.8 | Statistics

Where applicable, data are presented as the mean $\pm$ SEM with the number of independent biological replicates (n) indicated in the relevant figure panels. GraphPad Prism software version 6.0 was used to determine the significance of differences via the two-tailed Student's t-test (for comparisons between two groups) or two-way ANOVA (for comparisons between more than two groups). Differences were considered statistically significant when p-values were less than .05.

3 | RESULTS

3.1 | Spatiotemporal expression of FAM172A and CHD7 suggests a direct role in sex determination

To determine whether FAM172A and CHD7 proteins play an active role in sex determination, we first assessed their abundance in developing mouse gonads via immunofluorescence (Figure 1 and Figure S1). This analysis was performed using gonads of both sexes (as determined by PCR-based sexing), when sex determination occurs at e11.5 and the day after at e12.5. *Fam172a* and *Chd7* genes are both known to be widely expressed in developing embryos.[22,26,35] Accordingly, FAM172A and CHD7 proteins were detected throughout XX and XY gonads (GATA4-positive) and attached mesonephroi (Figure S1A–D). Specific staining for each protein was confirmed by a marked signal decrease in corresponding mutant mice (Figure S1E,F), which are either homozygous for a hypomorphic allele (*Fam172a^{Tp/Tp}*) or heterozygous for a null allele (*Chd7^{Gt/+}*). The extent of colocalization with GATA4, a well-known gonadal somatic cell marker,[36] was then evaluated in freshly dissociated gonads (with mesonephroi removed). This analysis revealed that virtually all GATA4-positive nuclei are also positive for FAM172A and CHD7, representing about half of all FAM172A-positive and CHD7-positive cells (Figure 1A–F). This proportion appeared initially similar at e11.5 in both sexes, but then became significantly dimorphic between males and females at e12.5 (Figure 1E,F). At this later stage, the relative proportion of FAM172A-positive and CHD7-positive cells also positive for GATA4 is decreased in female gonads, most likely because this somatic cell lineage does not expand as quickly in ovaries as it does in testes.[37] Considering that the GATA4-positive cell lineage is where the Sertoli-vs.-granulosa cell fate decision underlying testis-vs.-ovary development is taken,[38] the tissue distribution and subcellular localization of FAM172A and CHD7 thus suggest a direct and active role for both proteins in this process.

3.2 | The FAM172A interactome suggests roles in transcriptional and alternative splicing regulation during male sex determination and differentiation

In contrast to the CHD7 interactome that has been extensively studied in a variety of contexts,[39–43] we still know relatively little about FAM172A binding partners. Our previous analysis of neural crest-derived Neuro2a cells, mostly based on affinity-purification coupled to mass spectrometry,

revealed that the FAM172A interactome is especially enriched in chromatin proteins (including CHD7) and splicing regulators (including AGO2).[22] To verify whether the FAM172A interactome is similar in gonadal somatic cells, we thus decided to use the same pull-down approach and MBP-tagged version of FAM172A. Given the male-to-female sex reversal phenotype of *Fam172a^{Tp/Tp}* mice, we further reasoned that a pre-Sertoli cell line would be ideal to accommodate the large amounts of proteins required for such an experiment. To the best of our knowledge, such a cell line has only been successfully derived from genital ridges of pig embryos.[34] In accordance with our expression data (Figure 1), both FAM172A and CHD7 proteins were found to be present in these PGR9E11 cells (Figure S2), which are known to express many sex-determining genes such as *GATA4*, *NR5A1*, *SOX9*, and *SRY*.[34,44] Using a mammalian peptide database (which includes currently available *Sus scrofa* peptide sequences), our proteomics analysis revealed that the _MBP_FAM172A interactome in PGR9E11 pre-Sertoli cells is roughly similar to what was previously observed in neural crest-derived Neuro2a cells. As indicated in Table 1, this interactome notably includes chromatin proteins (e.g., Histones H2A, H2B, and H4), alternative splicing regulators (e.g., HNRNPAB and HNRNPU), and several nucleolus-enriched proteins (e.g., Nucleolin, Nucleophosmin, and many ribosomal proteins) that were also previously identified in the spliceosome interactome.[45] Although many targets were likely overlooked because of the incomplete nature of *Sus scrofa* protein databases and limited homology of some orthologs in other mammals, these proteomics data nonetheless strongly suggest that the roles of FAM172A in the regulation of transcriptional and alternative splicing outcomes are conserved in pre-Sertoli cells during sex determination and early sex differentiation.

3.3 | FAM172A and CHD7 can directly control *Sry/SRY* expression

Based on the partially penetrant but complete male-to-female sex reversal phenotype observed in CHARGE syndrome mouse models,[22] we next verified whether expression of the master sex-determining gene *Sry* was affected by the partial loss of either FAM172A or CHD7 (vs. WT controls of the same FVB/N genetic background). This analysis was performed at the critical time for male sex determination (e11.5), using tail somite (TS) counts for the accurate developmental staging of gonads. For both *Fam172a^{Tp/Tp}* and *Chd7^{Gt/+}* mutant mouse lines, whole-mount in situ hybridization revealed various degrees of *Sry* expression in TS18 male gonads, ranging from severely reduced to unaffected (Figure 2A). These results
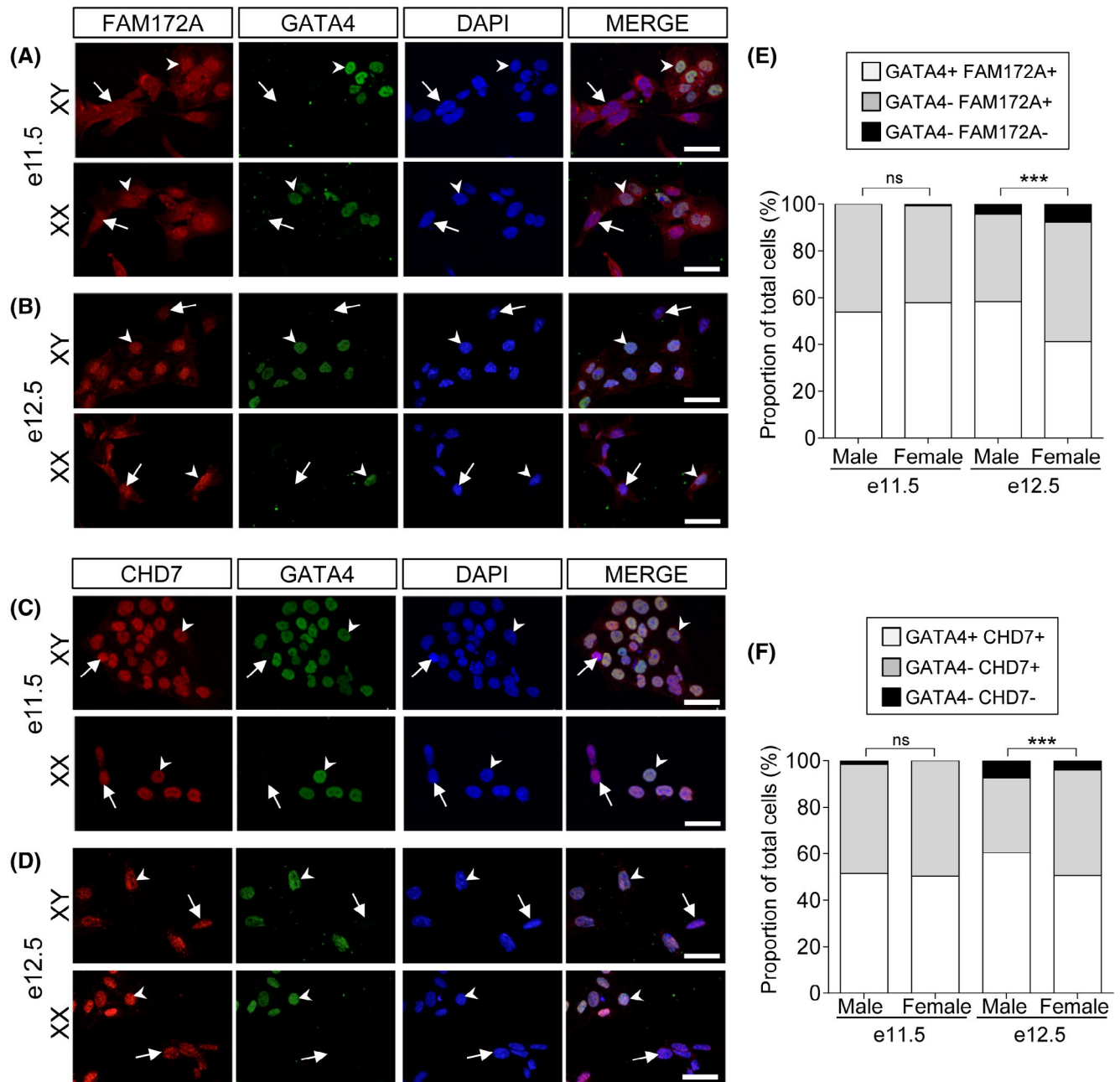
FIGURE 1 FAM172A and CHD7 distribution in developing gonads. (A–D) Representative images of freshly dissociated gonads from e11.5 and e12.5 wild-type embryos immunolabeled with antibodies against GATA4 (green) and either FAM172A or CHD7 (red), and counterstained with DAPI (blue). Arrowheads indicate double-positive cells for GATA4 and either FAM172A (A and B) or CHD7 (C and D), while arrows point to FAM172A-positive (A and B) or CHD7-positive (C and D) but GATA4-negative cells. (E and F) Quantitative analysis of cell counts based on images such as those displayed in corresponding panels on the left ($N = 3$ biological replicates, $n = 303$–647 cells per condition; ***$p < .001$; Chi-Square test). Scale bar, 50 μm

were confirmed using RT-qPCR, which further allowed us to distinguish between single-exon (*Sry-S*) and two-exon (*Sry-T*) transcripts (Figure 2B and Figure S3). Analysis of XY gonads before (TS13–15; Figure S3A), during (TS16–18; Figure 2B) and after (TS19–22; Figure S3B) the peak of *Sry* expression in the FVB/N background[27] revealed a general trend toward decreased levels of both isoforms,

without significant impact on the overall *Sry-S*:*Sry-T* ratio (0.72 ± 0.05 for WT; 0.65 ± 0.12 for *Fam172a*$^{Tp/Tp}$; 0.69 ± 0.04 for *Chd7*$^{Gt/+}$). As these expression data suggested a role in the fine-tuning of *Sry* transcription, we then evaluated the possibility of a direct regulation using ChIP-qPCR assays in PGR9E11 pre-Sertoli cells. Target regions in the pig *SRY* promoter were selected in part because they were

TABLE 1 FAM172A-interacting proteins in PGR9E11 cells

Protein name	Gene name	Accession #	MW	emPAI
Glyceraldehyde-3-phosphate dehydrogenase	*Gapdh*	P16858	36	0.902
Pyruvate kinase PKM	*Pkm*	P52480	58	0.884
40S ribosomal protein S3	*Rps3*	P62908	27	0.687
Heat shock protein HSP 90-beta	*Hsp90ab1*	P11499	83	0.681
Peptidyl-prolyl cis-trans isomerase A	*Ppia*	P17742	18	0.648
Peroxiredoxin-1	*Prdx1*	P35700	22	0.630
Heat shock protein HSP 90-alpha	*Hsp90aa1*	P07901	85	0.621
40S ribosomal protein S4, X isoform	*Rps4x*	P62702	30	0.529
Heterogeneous nuclear ribonucleoprotein A/B	*Hnrnpab*	Q99020	31	0.498
Tubulin alpha-1A chain	*Tuba1a*	P68369	50	0.487
Histone H2A type 1-B/E	*Hist1h2ab*	C0HKE1	14	0.439
40S ribosomal protein S18	*Rps18*	P62270	18	0.422
Histone 4	*Hist1h4a*	P62806	11	0.384
Elongation factor 1-alpha 1	*Eef1a1*	P10126	50	0.369
Galectin-1	*Lgals1*	P16045	15	0.354
10 kDa heat shock protein	*Hspe1*	Q64433	11	0.346
Actin, alpha cardiac muscle 1	*Actc1*	P68033	42	0.322
40S ribosomal protein S25	*Rps25*	P62852	14	0.306
14-3-3 protein zeta/delta	*Ywhaz*	P63101	28	0.296
40S ribosomal protein S16	*Rps16*	P14131	16	0.295
Histone H2B type 1-A	*Hist1h2ba*	P70696	14	0.288
40S ribosomal protein S15a	*Rps15a*	P62245	15	0.281
14-3-3 protein epsilon	*Ywhae*	P62259	29	0.257
ATP synthase subunit alpha	*Atp5a1*	Q03265	55	0.255
40S ribosomal protein S7	*Rps7*	P62082	22	0.251
Ras-related protein Rab-10	*Rab10*	P61027	23	0.245
60S ribosomal protein L22	*Rpl22*	P67984	15	0.245
Tubulin beta-5 chain	*Tubb5*	P99024	50	0.245
Ras-related protein Rab-1A	*Rab1a*	P62821	23	0.244
L-lactate dehydrogenase A	*Ldha*	P06151	36	0.233
Nucleophosmin	*Npm1*	Q61937	33	0.225
Elongation factor 1-beta	*Eef1b*	O70251	25	0.221
Actin, cytoplasmic 1	*Actb*	P60710	42	0.214
40S ribosomal protein S13	*Rps13*	P62301	17	0.205
40S ribosomal protein S11	*Rps11*	P62281	18	0.199
Alpha-enolase	*Eno1*	P17182	47	0.192
T-complex protein 1 subunit delta	*Cct4*	P80315	58	0.151
Cofilin-1	*Cfl1*	P18760	18	0.143
Actin	*Actb*	P60710	42	0.141
60S ribosomal protein L23a	*Rpl23a*	P62751	18	0.140
Thioredoxin	*Txn*	P10639	12	0.140
GTP-binding nuclear protein Ran	*Ran*	P62827	24	0.139

(Continues)

TABLE 1 (Continued)

Protein name	Gene name	Accession #	MW	emPAI
ATP synthase subunit beta	Atp5b	P56480	52	0.121
Lithostathine	Reg1	P47137	32	0.119
Alpha-2-macroglobulin	A2m	Q6GQT1	61	0.113
Ubiquitin-60S ribosomal protein L40	Uba52	P62984	6	0.109
Profilin-1	Pfn1	P62962	15	0.107
40S ribosomal protein S4	Rps4x	P62702	30	0.100
Endoplasmic reticulum resident protein 27	Erp27	Q9D8U3	28	0.097
Elongation factor 1-alpha 1	Eef1a1	P10126	50	0.089
T-complex protein 1 subunit beta	Cct2	P80314	57	0.086
Fructose-bisphosphate aldolase A	Aldoa	P05064	39	0.083
Elongation factor 2	Eef2	P58252	95	0.082
60 kDa heat shock protein	Hspd1	P63038	58	0.081
60S ribosomal protein L31	Rpl31	P62900	14	0.074
60S ribosomal protein L35	Rpl35	Q6ZWV7	15	0.074
Transitional endoplasmic reticulum ATPase	Vcp	Q01853	89	0.073
GTP-binding protein Di-Ras2	Diras2	Q5PR73	22	0.072
ADP/ATP translocase 3	Arl2	Q9D0J4	21	0.048
Calnexin	Canx	P35564	65	0.047
Heat shock cognate 71 kDa protein	Hspa8	P63017	71	0.044
Vimentin	Vim	P20152	54	0.041
Eukaryotic initiation factor 4A-I	Eif4a1	P60843	46	0.034
Heat shock 70 kDa protein 4	Hspa4	Q61316	94	0.033
Protein disulfide-isomerase A3	Pdia3	P27773	54	0.027
Nucleolin	Ncl	Q9FVQ1	59	0.025
Heterogeneous nuclear ribonucleoprotein U	Hnrnpu	Q8VEK3	88	0.021
GAS2-like protein 1	Gas2l1	Q8JZP9	72	0.013
Ribosome-releasing factor 2	Gfm2	Q8R2Q4	86	0.012
Coiled-coil domain-containing protein 136	Ccdc136	Q3TVA9	32	0.006

Note: Proteins were included if enriched at least 1.5-fold in comparison to the MBP negative control and detected in at least two out of the three biological replicates of this analysis. The indicated emPAI (exponentially modified Protein Abundance Index) value corresponds to the average of the three biological replicates. Accession number is for the Uniprot database.

known to be bound by the sex-determining transcription factors NR5A1 (SF1), WT1, and GATA4.[34,44] Moreover, corresponding sequences of murine *Sry* were known to be occupied by regulators of H3K9 methylation,[5,6] a finding of particular relevance given that the H3K9 methyltransferase G9A (also known as EHMT2) and the H3K9 demethylase JMJD1C were also previously identified as FAM172A binding partners in Neuro2a cells.[22] In line with this, our ChIP-qPCR results revealed that both FAM172A and CHD7 were present on the most distal tested region of the *SRY* promoter (Figure 2C). These data thus suggest that FAM172A and CHD7 can directly control male sex determination, at least in part by modulating *Sry/SRY* gene transcription.

3.4 | FAM172A and CHD7 are necessary for proper transcriptional regulation during early male sex differentiation

To verify whether FAM172A and CHD7 might have additional roles in male sex differentiation downstream of *Sry*, we then analyzed the transcriptome of $Fam172a^{Tp/Tp}$ and $Chd7^{Gt/+}$ pre-Sertoli cells isolated from e12.5 embryos that have successfully undergone male sex determination—based on the presence of male-specific coelomic vessel and testis cords (i.e., non-sex-reversed). High-throughput RNA-seq experiments were realized by taking advantage of the *Gata4p[5kb]-RFP* transgene (hereafter referred to as *G4-RFP*), which is specifically active in testes (in the Sertoli
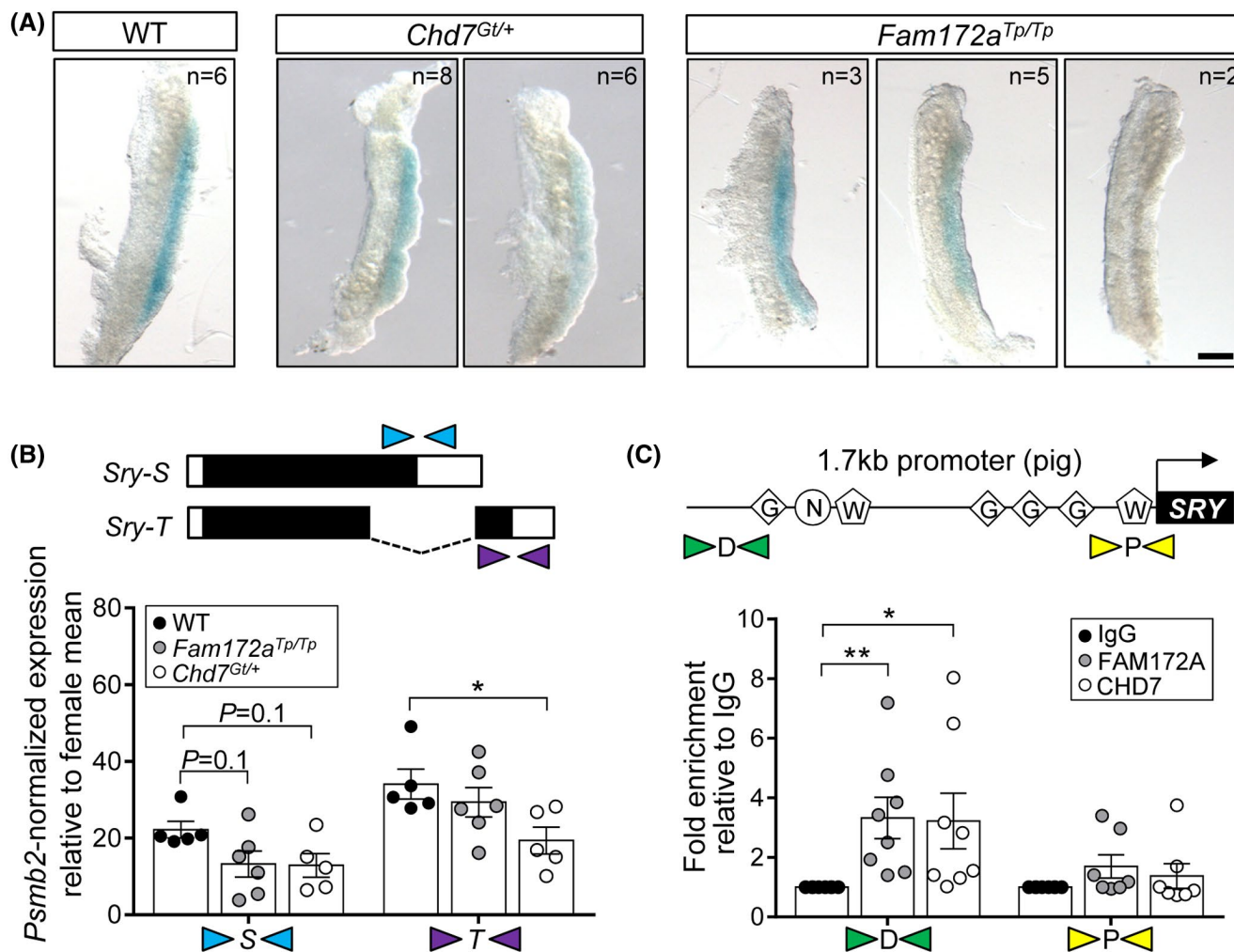
FIGURE 2 *Sry* is a direct target of FAM172A and CHD7 during sex determination. (A) Whole-mount in situ hybridization of *Sry* transcripts in XY gonads from stage-matched (TS18) wild-type, *Fam172a*[Tp/Tp] and *Chd7*[Gt/+] embryos. The numbers of gonads with representative expression levels are indicated in the upper right corner. Scale bar, 200 μm. (B) RT-qPCR analysis of *Sry-S* and *Sry-T* expression levels in pairs of XY gonads from stage-matched (TS16-18) wild-type, *Fam172a*[Tp/Tp] and *Chd7*[Gt/+] embryos ($N = 5–6$ biological replicates, $*p < .05$; 2-way ANOVA and Tukey's multiple comparison test). Black and white boxes indicate coding and untranslated regions, respectively. (C) FAM172A and CHD7 ChIP-qPCR assays for distal (D) and proximal (P) regions of the pig *SRY* promoter in PGR9E11 cells ($N = 8$ biological replicates, $**p < .01$, $*p < .05$; 2-way ANOVA and Tukey's multiple comparison test). W, WT1 binding site; G, GATA4 binding site, N, NR5A1/SF-1 binding site
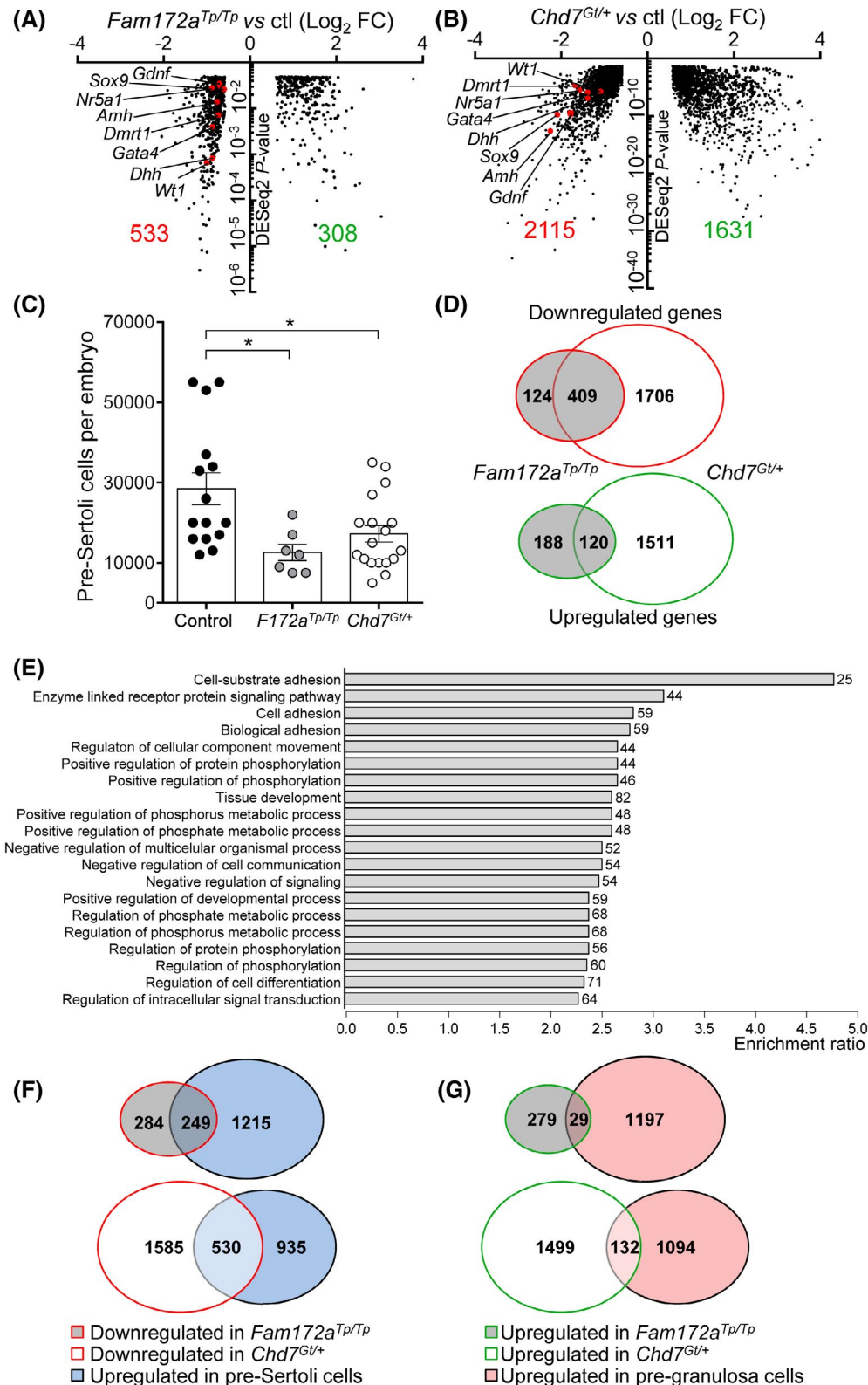
cell lineage) and not in ovaries.[27] The *G4-RFP* transgene was introduced in each mutant line by breeding, thereby allowing to confirm proper male sex determination of selected e12.5 testes (TS22-25) and to specifically recover pre-Sertoli cells via fluorescence-activated cell sorting (FACS). When compared to *G4-RFP* controls using the DESeq pipeline, 841 and 3746 transcriptional targets (using 1.5-fold change and $p < .05$ as cut-off values) were found to be affected in *Fam172a*[Tp/Tp];*G4-RFP* and *Chd7*[Gt/+];*G4-RFP* pre-Sertoli cells, respectively (Figure 3A,B and Datasets S1 and S2). Strikingly, despite the marked difference in the total number of affected genes (most likely due to the exclusion of one *Fam172a*[Tp/Tp];*G4-RFP* sample that failed quality control, making our significance cut-off values

harder to reach; see Section 2), downregulated genes included a common set of 8 genes with known key roles in male sex determination/differentiation (in alphabetical order): *Amh*, *Dhh*, *Dmrt1*, *Gata4*, *Gdnf*, *Nr5a1*, *Sox9*, and *Wt1*. In accordance with the prominent role of many of these genes in the differentiation and expansion of the Sertoli cell lineage, FACS-based cell counting revealed that gonads from *Fam172a*[Tp/Tp];*G4-RFP* and *Chd7*[Gt/+];*G4-RFP* embryos generally contained fewer RFP-positive cells than in *G4-RFP* controls (Figure 3C).

Yet, the overlap between both mutant transcriptomes far exceeded this handful of key genes, notably covering 77% (409/533 genes) and 19% (409/2115 genes) of all downregulated genes in *Fam172a*[Tp/Tp];*G4-RFP* and *Chd7*[Gt/+];*G4-RFP*

pre-Sertoli cells, respectively (Figure 3D and Dataset S3). Gene ontology (GO) analysis of this common set of downregulated genes (top 20 most enriched GO terms at FDR ≤0.05) revealed a particular enrichment for genes playing roles in the regulation of cell adhesion (3/20 GO terms), cell signaling (4/20 GO terms), and protein phosphorylation

(8/20 GO terms) (Figure 3E). The overlap appeared much less pronounced in the case of upregulated genes, covering 39% (120/308 genes) and 7% (120/1631 genes) of corresponding gene sets from $Fam172a^{Tp/Tp}$;G4-RFP and $Chd7^{Gt/+}$;G4-RFP mutants, respectively (Figure 3D and Dataset S3). Accordingly, GO analysis of this common set of upregulated

(A) $Fam172a^{Tp/Tp}$ vs ctl (Log$_2$ FC)

(B) $Chd7^{Gt/+}$ vs ctl (Log$_2$ FC)

(C)

(D) Downregulated genes

(E)

(F)
- ▣ Downregulated in $Fam172a^{Tp/Tp}$
- ▢ Downregulated in $Chd7^{Gt/+}$
- ▣ Upregulated in pre-Sertoli cells

(G)
- ▣ Upregulated in $Fam172a^{Tp/Tp}$
- ▢ Upregulated in $Chd7^{Gt/+}$
- ▣ Upregulated in pre-granulosa cells

genes yielded no statistically significant enrichment for any biological process (Figure S4). Interestingly, comparison of our RNA-seq datasets with previously reported microarray datasets of differentially expressed genes in pre-Sertoli and pre-granulosa cells at e12.5[46] further revealed that a large subset of downregulated genes in both $Fam172a^{Tp/Tp}$;G4-RFP (47%; 249/533 genes) and $Chd7^{Gt/+}$;G4-RFP (25%; 530/2115 genes) transcriptomes are normally up-regulated in pre-Sertoli cells (Figure 3F and Dataset S3). Conversely, only a small subset of the upregulated genes in $Fam172a^{Tp/Tp}$;G4-RFP (9%; 29/308 genes) and $Chd7^{Gt/+}$;G4-RFP (8%; 132/1631 genes) pre-Sertoli cells were previously identified as normally up-regulated in pre-granulosa cells (Figure 3G and Dataset S3). All these observations are thus consistent with the notion that FAM172A and CHD7 are required for fine-tuning the transcriptional landscape of pre-Sertoli cells during early sex differentiation in order to fully adopt a male fate and prevent partial adoption of a female fate.

3.5 | FAM172A and CHD7 are important for alternative splicing accuracy during early male sex differentiation

Using the rMATS pipeline to detect alternatively spliced variants, we identified 487 and 1046 aberrantly spliced transcripts (using $p < .05$ and variation in inclusion level >0.1 as cut-off values) in $Fam172a^{Tp/Tp}$;G4-RFP and $Chd7^{Gt/+}$;G4-RFP pre-Sertoli cells, respectively (Figure 4A,B and Datasets S4 and S5). As previously observed in neural crest cells,[22] the majority of splicing events affected by the loss of FAM172A and CHD7 were either of the Skipped exon (54% [265/487] and 40% [414/1046], respectively) or Retained intron (19% [92/487] and 42% [438/1046], respectively) categories. At the gene level (accounting for the fact that some genes have multiple aberrantly spliced variants), we observed a much greater overlap between misspliced and misexpressed gene sets in $Chd7^{Gt/+}$;G4-RFP (32%; 269/842 misspliced genes) than in $Fam172a^{Tp/Tp}$;G4-RFP (6%; 26/425 misspliced genes) mutants (Figure 4C,D and Dataset S3). Yet, a common set of 188 alternatively spliced transcripts was found to be

affected in both mutants, representing 39% (188/487 splicing events) and 18% (188/1046 splicing events) of all dysregulated splicing events in $Fam172a^{Tp/Tp}$;G4-RFP and $Chd7^{Gt/+}$;G4-RFP pre-Sertoli cells, respectively (Figure 4E and Dataset S3). Moreover, the vast majority of these shared alternatively spliced transcripts were similarly dysregulated in terms of increased-vs.-decreased inclusion levels (85%; 160/188 splicing events) (Figure 4F and Dataset S3). Interestingly, GO analysis of these similarly dysregulated transcripts in both mutants (top 10 most enriched GO terms at FDR ≤0.05) revealed a particular enrichment for genes involved in cell adhesion (2/10 GO terms), actin-based structure organization (3/10 GO terms), and protein-containing complex assembly (2/10 GO terms) (Figure 4G).

$Wt1$ and $Frfr2$ were not found in the set of co-regulated alternatively spliced transcripts. However, close examination of our datasets revealed that each mutant had an aberrantly spliced variant of a distinct WNT effector-coding gene that fell into the skipped exon category. Compared to control G4-RFP pre-Sertoli cells, $Lef1$ variable exon 6 was found to be less frequently included in $Fam172a^{Tp/Tp}$;G4-RFP mutants while $Tcf7l2$ variable exon 6 (also referred to as exon 4a in prior work[47]) was found to be more frequently included in $Chd7^{Gt/+}$;G4-RFP mutants (Figure 5A and Datasets S4 and S5). Although completely different in terms of affected genes and nature of changes (decreased vs. increased inclusion levels), both splicing events caught our attention because of their presumed similar negative impact on the transcriptional output of canonical WNT signaling, a key pathway for both female and male gonad formation.[19,20] Indeed, LEF1 protein lacking exon 6 was previously described to have decreased β-catenin-dependent transactivation capacity[18] whereas TCF7L2 protein including exon 6 (exon 4a) was previously described to have increased Groucho-dependent transrepression capacity.[47] To verify the possibility of direct regulation of these splicing events by FAM172A and CHD7, we analyzed their presence on corresponding chromatin regions in PGR9E11 cells by ChIP-qPCR. In both cases, FAM172A (on $LEF1$ exon 6) and CHD7 (on $TCF7L2$ exon 6) were found to preferentially occupy the alternatively spliced exon in comparison to a constant (i.e., non-alternatively spliced) exon

---

FIGURE 3 FAM172A and CHD7 are important regulators of the pre-Sertoli cell transcriptome during early sex differentiation. (A and B) Volcano plots summarizing the RNA-seq–based analysis of differential gene expression levels in e12.5 pre-Sertoli cells recovered from G4-RFP (control), $Fam172a^{Tp/Tp}$;G4-RFP (A) and $Chd7^{Gt/+}$;G4-RFP (B) testes. Only genes modulated at least 1.5-fold compared to control and with a p-value below .05 are displayed. Red numbers indicate the total number of downregulated genes, green numbers indicate the total number of upregulated genes, and red dots represent known critical regulators of sex differentiation. (C) The number of RFP-positive pre-Sertoli cells recovered by FACS from G4-RFP (control), $Fam172a^{Tp/Tp}$;G4-RFP and $Chd7^{Gt/+}$;G4-RFP e12.5 testes. (D) Venn diagrams comparing downregulated (upper panel) and upregulated (lower panel) genes between $Fam172a^{Tp/Tp}$;G4-RFP and $Chd7^{Gt/+}$;G4-RFP datasets. (E) GO analysis (FDR ≤0.05) of all genes downregulated in both $Fam172a^{Tp/Tp}$;G4-RFP and $Chd7^{Gt/+}$;G4-RFP datasets. (F and G) Venn diagrams comparing downregulated (F) or upregulated (G) genes in $Fam172a^{Tp/Tp}$;G4-RFP and $Chd7^{Gt/+}$;G4-RFP mutants with genes normally upregulated in e12.5 pre-Sertoli (F) or pre-granulosa (G) cells as previously reported[46]
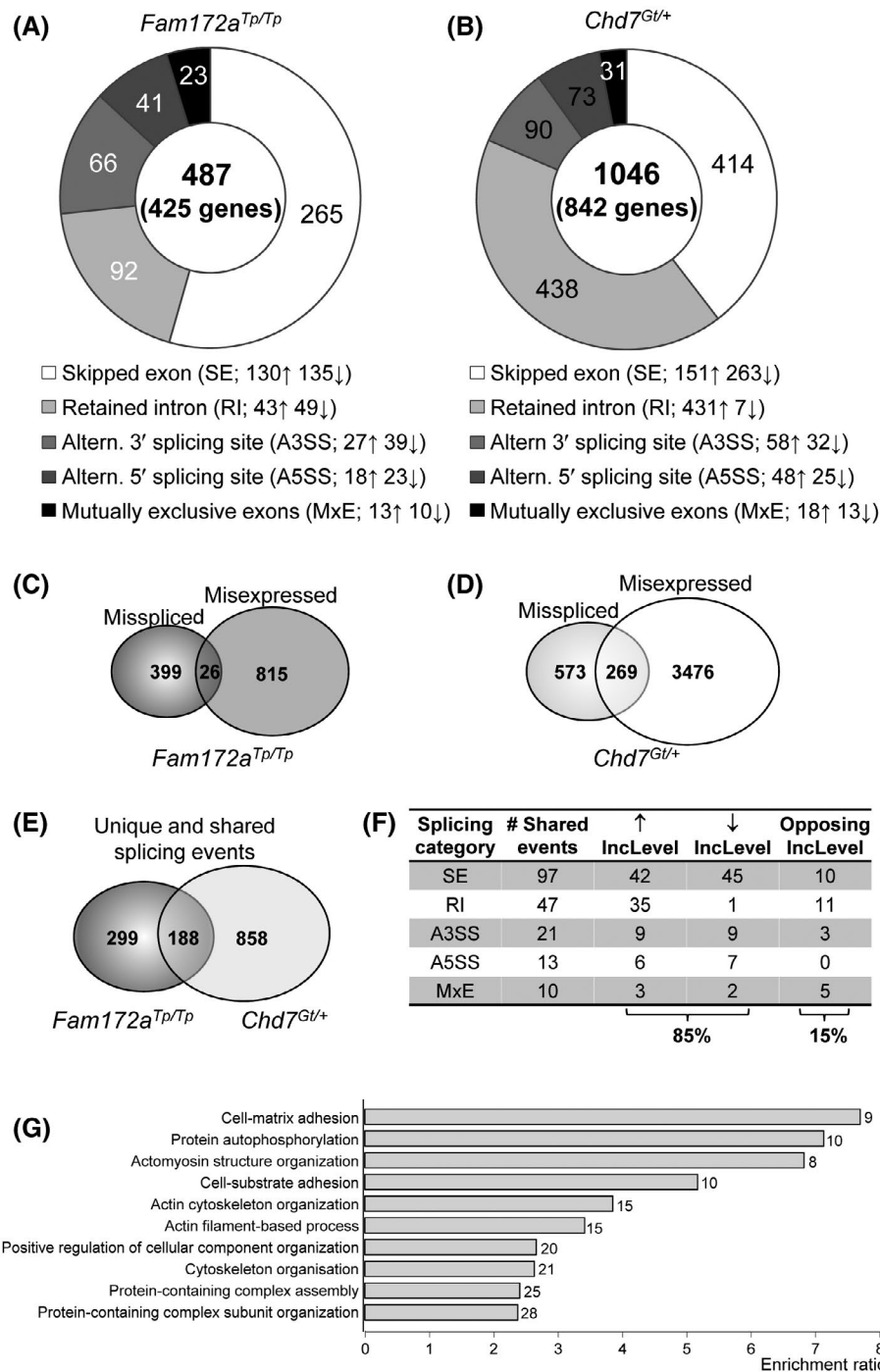
FIGURE 4 FAM172A and CHD7 are important for splicing accuracy in pre-Sertoli cells. (A and B) Donut chart showing the distribution of all differentially modulated alternative splicing events in e12.5 pre-Sertoli cells from $Fam172a^{Tp/Tp}$;G4-RFP (A; 487 events affecting 425 genes) and $Chd7^{Gt/+}$;G4-RFP (B; 1046 events affecting 842 genes) embryos. (C and D) Comparison of misspliced and misexpressed gene sets for $Fam172a^{Tp/Tp}$;G4-RFP (C) and $Chd7^{Gt/+}$;G4-RFP (D) mutants. (E) Comparison of all dysregulated splicing events between $Fam172a^{Tp/Tp}$;G4-RFP and $Chd7^{Gt/+}$;G4-RFP mutants. (F) Detailed overview of splicing events dysregulated in both $Fam172a^{Tp/Tp}$;G4-RFP and $Chd7^{Gt/+}$;G4-RFP mutants, per splicing category and direction of inclusion level. (G) GO analysis (FDR ≤0.05) of all genes misspliced in the same direction for both $Fam172a^{Tp/Tp}$;G4-RFP and $Chd7^{Gt/+}$;G4-RFP mutants

(Figure 5B,C). These results thus strongly suggest that FAM172A and CHD7 can similarly influence the transcriptional output of canonical WNT signaling in pre-Sertoli cells through distinct alternative splicing-dependent mechanisms. We interpret this as meaning that the lower levels of WNT signaling in male gonads compared to female gonads are most likely further decreased in mutant males. These data could explain, at least in part, the
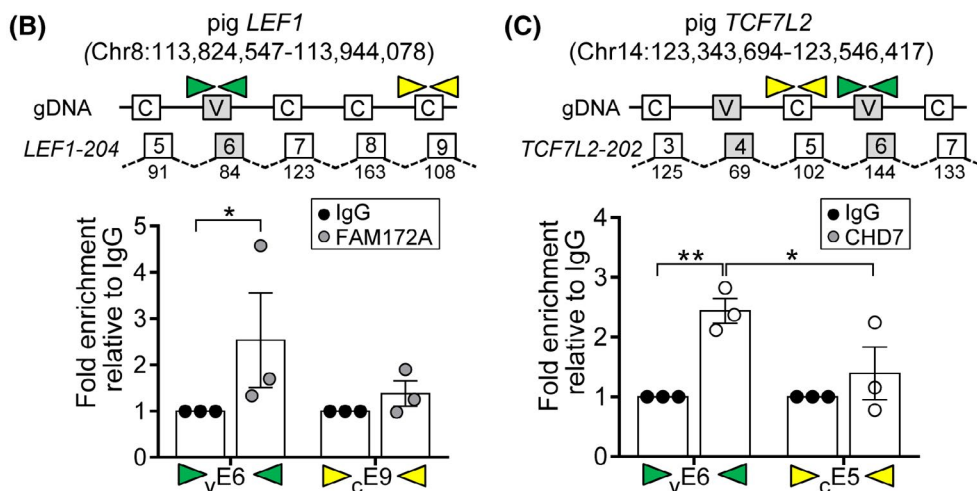
FIGURE 5 Alternative splicing of WNT effector genes is directly regulated by FAM172A and CHD7. (A) Detailed information about the alternative exons of *Lef1* and *Tcf7l2* that are misspliced in *Fam172a*$^{Tp/Tp}$;*G4-RFP* and *Chd7*$^{Gt/+}$;*G4-RFP* pre-Sertoli cells, respectively. (B and C) FAM172A (B) and CHD7 (C) ChIP-qPCR assays for the affected variable exon (v in gDNA view) relative to a constant exon (c in gDNA view) of pig *LEF1* (B) and *TCF7L2* (C) genes in PGR9E11 cells (N = 3 biological replicates; **p ≤ .01, *p ≤ .05; Student's *t*-test). For each gene, exon numbers are based on the indicated transcript name, with exon size (in bp) indicated under each exon

observed transcriptional downregulation of *Gdnf* and *Amh* (Figure 3A,B)—two genes that have been reported as direct targets of canonical WNT signaling in Sertoli cells.[48]

3.6 | Loss of FAM172A and CHD7 negatively impacts the morphology of seminiferous tubules in adult mice

WNT signaling and many other co-regulated transcriptional targets of FAM172A and CHD7 (e.g., *Dhh*, *Gata4*, *Sox9*, and *Wt1*) in pre-Sertoli cells are known to control testis cord formation right after sex determination.[49,50] Furthermore, the gene regulatory network formed by these FAM172A/CHD7-target genes also ensures long-term maintenance of proper testis cord morphology,[49] at least in part by regulating the expression of another set of genes coding for key components of the collagen-enriched extra-cellular matrix that is deposited by Sertoli cells around testis cords.[49,51] This, along with the fact that "cell-substrate adhesion" (Figure 3E) and "cell-matrix adhesion" (Figure 4G) were the top GO terms associated with transcriptional and alternative splicing targets of FAM172A and CHD7 (which notably include several collagen and integrin isoforms; Dataset S3), prompted us to

examine the impact of their partial loss on the morphology of seminiferous tubules in adult mice. In accordance with their transcriptional and alternative splicing signature, analysis of hematoxylin/eosin-stained sections of 2-month-old testes revealed the presence of misshapen tubules in *Fam172a*$^{Tp/Tp}$ and *Chd7*$^{Gt/+}$ mutants (Figure 6A). In contrast to WT seminiferous tubules that constantly appear circular with a smooth lining of basal lamina when cross-sectioned, we found that mutant seminiferous tubules were generally less circular and frequently had an irregular lining (Figure 6A). Using immunofluorescence, we further validated that these morphological defects were associated with the reduced amount and uneven distribution of COL4 around seminiferous tubules (Figure 6B) and ITGA6 in Sertoli cells (Figure 6C)—these proteins being some of the collagen and integrin isoforms found to be transcriptionally downregulated in *Fam172a*- and *Chd7*-mutant pre-Sertoli cells (Dataset S3).

4 | DISCUSSION

Taking advantage of two genetically distinct CHARGE syndrome mouse models displaying partially penetrant but complete male-to-female sex reversal, we identified the
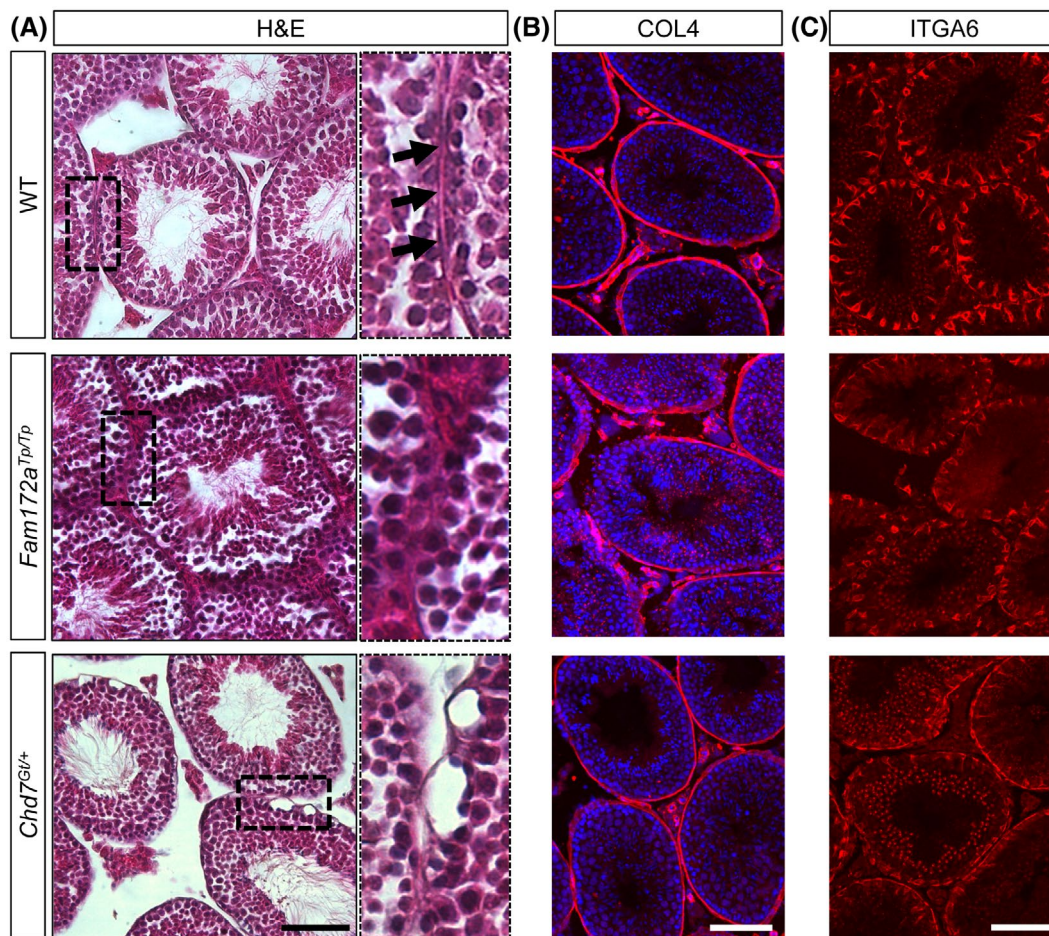
FIGURE 6 Loss of FAM172A and CHD7 is associated with morphological abnormalities of seminiferous tubules in adult testes. (A) Hematoxylin and eosin double-stained cross-sections of adult testes (2-month-old) showing irregular lining and decreased roundness of seminiferous tubules of mutant animals (middle and lower panels for *Fam172a*$^{Tp/Tp}$ and *Chd7*$^{Gt/+}$, respectively) in comparison to wild-type controls (upper panels). (B and C) Immunofluorescence staining of cross-sections of adult testes (2-month-old) showing thinner/irregular COL4 signal (red) around mutant seminiferous tubules (B; counterstained with DAPI) and weaker/uneven ITGA6 signal (red) in Sertoli cells (C). All images are representative of $N = 3$ animals. Scale bar, 100 μm

co-transcriptional regulator FAM172A and the chromatin remodeler CHD7 as new players in the gene regulatory network of male sex determination and differentiation of pre-Sertoli cells. FAM172A and CHD7 appear to co-regulate both of these processes through chromatin-dependent control of transcription and alternative splicing, as we previously observed in neural crest cells.[22] Findings from the current study thus strengthen the link between chromatin-dependent transcriptional mechanisms and sex determination and add a new regulatory layer to the link between alternative splicing and sex determination/differentiation. This work also potentially has clinical relevance with regards to the genital abnormalities associated with CHARGE syndrome.

Our analyses of mouse gonads and pig pre-Sertoli cells around the time of sex determination suggest that both FAM172A and CHD7 directly occupy and regulate the promoter of the male-determining gene *Sry/SRY* (Figure 2 and Figure S3). Consistent with a role in fine-tuning promoter

activity through the control of chromatin features, partial loss of either FAM172A (in hypomorphic *Fam172a*$^{Tp/Tp}$ mutants) or CHD7 (in heterozygous *Chd7*$^{Gt/+}$ mutants) in the FVB/N background was associated with variable degrees of *Sry* downregulation in male gonads. This general pattern was observed for both *Sry-S* and *Sry-T* transcripts, throughout the temporal window of *Sry* expression in the FVB/N genetic background.[27] Although we cannot exclude the possibility that other relevant target genes might also be affected, these data suggest that the inability to properly upregulate *Sry* transcription above a critical threshold[52] is the main reason for the observed male-to-female sex reversal in a subset of animals from both mutant lines.[22]

As FAM172A is known to physically interact with both positive and negative regulators of H3K9 methylation,[22] our findings are also consistent with the previously described key role of this repressive histone mark in the control of *Sry* gene expression and associated male sex

determination.[5,6] CHD7-mediated regulation of *Sry* most likely involves a distinct, but complementary, mechanism. Indeed, CHD7 is known to preferentially occupy genomic regions enriched in methylated H3K4,[25] and activating histone mark that is presumably deposited upon demethylation of H3K9 at the *Sry* promoter.[5,6] In line with these observations, it is interesting to note that fully sex-reversed XY females appear to be similarly subfertile when lacking either FAM172A (to be described elsewhere) or the H3K9 demethylase JMJD1A.[5] Moreover, in both cases, the sex reversal phenotype is influenced by the genetic background, being markedly reduced in frequency (from 88% to 14% in the case of *Jmjd1a*-deficient mice[5]) or eliminated (from 25% to 0% in the case of *Fam172a*-deficient mice; data not shown) when maintained in a C57BL/6 background.

High-throughput analysis of non-sex-reversed embryonic testes soon after the critical stage of *Sry*-dependent sex determination allowed us to discover many other co-regulated targets at both transcriptional and alternative splicing levels (Figures 3 and 4). The overlap was especially striking in the case of transcriptionally downregulated genes (408 genes), representing 77% and 19% of all genes showing decreased expression upon the loss of FAM172A and CHD7, respectively (Figure 3). The overlap was also extensive in the case of dysregulated splicing events (188 events in total), representing 38% and 19% of all splicing events affected by the loss of FAM172A and CHD7, respectively (Figure 4). Deciphering the extent of direct vs. indirect regulation by FAM172A/CHD7 will require further studies, but the fact that our datasets of co-regulated targets include some genes coding for transcription (including known key regulators of pre-Sertoli cell fate like *Dmrt1*, *Gata4*, *Nr5a1*, *Sox9*, and *Wt1*), chromatin (including *Brd2* and *Kmt2d*) and splicing (including *Rsrc2* and *Rbm25*) factors provides a rationale for indirect regulation. Yet, the studied stage (i.e., right after sex determination) might be too early to detect the impact of these intermediate factors. In agreement with this, cross-comparison of our common set of 188 alternative splicing events at e12.5 with the published dataset of 154 SOX9-regulated alternative splicing events at e13.5[21] retrieved only one dysregulated event (a skipped exon for *Zmym4*) – an observation that should nonetheless be interpreted with caution given that outcomes of alternative splicing vary in a stage-dependent manner during progression through sex determination and differentiation.[12,13] It is also important to bear in mind that FAM172A and CHD7 roles can overlap without sharing the same target genes, as well exemplified by our finding of differential, but functionally convergent, regulation of *Lef1/LEF1* splicing by FAM172A and *Tcf7l2/TCF7L2* splicing by CHD7 (Figure 5).

The concomitant downregulation of multiple critical regulators (e.g., DHH, GATA4, SOX9, WNT, and WT1)

and effectors (e.g., collagens and integrins) of testis cord maintenance offers a plausible explanation for the mis-shapen seminiferous tubules observed in *Fam172a*- and *Chd7*-deficient post-natal testes (Figure 6). Together with the reduced number of pre-Sertoli cells observed at e12.5 (Figure 3C), this phenotype might also help to explain the smaller testes and decreased fertility rates displayed by a subset of adult *Fam172a*[Tp/Tp22] and *Chd7*[Whi/+53] mutant males. Indeed, although the functional consequence of the observed morphological phenotype in *Fam172a*- and *Chd7*-deficient testes is currently unknown, it is tempting to speculate that some germ cells might evade damaged tubules and get lost in the testis stroma as it has been described by others in *Dhh*- and *Wt1*-mutant mice.[49,51,54] This intriguing possibility would challenge the current view that genital anomalies in CHARGE syndrome are strictly due to dysfunction of the hypothalamus-pituitary-gonadal axis and associated delayed/arrested puberty.[55] Our data in mice combined with the fact that genital anomalies seem to be more frequently encountered in male patients (65% of boys vs. 21% of girls in studies reporting such anomalies in a sex-stratified manner)[56–64] suggest the presence of additional and potentially overlooked male-specific problems unrelated to hypothalamus-pituitary dysfunction in individuals affected by CHARGE syndrome. Taking this possibility into account might be important when comes time to consider hormone-based therapies, which seem to work well in *CHD7* mutation-positive individuals displaying isolated hypogonadotropic hypogonadism but less in patients displaying the full spectrum of CHARGE anomalies.[55]

DISCLOSURES

The authors declare no conflict of interest.

AUTHOR CONTRIBUTIONS

Nicolas Pilon conceived and supervised the study; Catherine Bélanger and Nicolas Pilon designed the experiments; Catherine Bélanger, Tatiana Cardinal, and Elizabeth Leduc performed the experiments and collected data; All authors analyzed and interpreted data; Catherine Bélanger, Robert S. Viger, and Nicolas Pilon drafted and edited the manuscript; All authors revised the manuscript.

DATA AVAILABILITY STATEMENT

The data that support the findings of this study are available in the methods, results and/or supplementary material of this article.

ORCID

Nicolas Pilon https://orcid.org/0000-0003-3641-0776

REFERENCES

1. Capel B. Vertebrate sex determination: evolutionary plasticity of a fundamental switch. *Nat Rev Genet*. 2017;18:675-689.
2. Stevant I, Nef S. Genetic control of gonadal sex determination and development. *Trends Genet*. 2019;35:346-358.
3. Garcia-Moreno SA, Plebanek MP, Capel B. Epigenetic regulation of male fate commitment from an initially bipotential system. *Mol Cell Endocrinol*. 2018;468:19-30.
4. Kuroki S, Tachibana M. Epigenetic regulation of mammalian sex determination. *Mol Cell Endocrinol*. 2018;468:31-38.
5. Kuroki S, Matoba S, Akiyoshi M, et al. Epigenetic regulation of mouse sex determination by the histone demethylase Jmjd1a. *Science*. 2013;341:1106-1109.
6. Kuroki S, Okashita N, Baba S, et al. Rescuing the aberrant sex development of H3K9 demethylase Jmjd1a-deficient mice by modulating H3K9 methylation balance. *PLoS Genet*. 2017;13:e1007034.
7. Bao L, Tian C, Liu S, et al. The Y chromosome sequence of the channel catfish suggests novel sex determination mechanisms in teleost fish. *BMC Biol*. 2019;17:6.
8. Deveson IW, Holleley CE, Blackburn J, et al. Differential intron retention in Jumonji chromatin modifier genes is implicated in reptile temperature-dependent sex determination. *Sci Adv*. 2017;3:e1700731.
9. Domingos JA, Budd AM, Banh QQ, Goldsbury JA, Zenger KR, Jerry DR. Sex-specific dmrt1 and cyp19a1 methylation and alternative splicing in gonads of the protandrous hermaphrodite barramundi. *PLoS One*. 2018;13:e0204182.
10. Qiu C, Zhang Y, Fan YJ, et al. HITS-CLIP reveals sex-differential RNA binding and alterative splicing regulation of SRm160 in Drosophila. *J Mol Cell Biol*. 2019;11:170-181.
11. Zheng ZZ, Sun X, Zhang B, et al. Alternative splicing regulation of doublesex gene by RNA-binding proteins in the silkworm Bombyx mori. *RNA Biol*. 2019;16:809-820.
12. Planells B, Gomez-Redondo I, Pericuesta E, Lonergan P, Gutierrez-Adan A. Differential isoform expression and alternative splicing in sex determination in mice. *BMC Genom*. 2019;20:202.
13. Zhao L, Wang C, Lehman ML, et al. Transcriptomic analysis of mRNA expression and alternative splicing during mouse sex determination. *Mol Cell Endocrinol*. 2018;478:84-96.
14. Hammes A, Guo JK, Lutsch G, et al. Two splice variants of the Wilms' tumor 1 gene have distinct functions during sex determination and nephron formation. *Cell*. 2001;106:319-329.
15. Bagheri-Fam S, Bird AD, Zhao L, et al. Testis determination requires a specific FGFR2 isoform to repress FOXL2. *Endocrinology*. 2017;158:3832-3843.
16. Kim Y, Bingham N, Sekido R, Parker KL, Lovell-Badge R, Capel B. Fibroblast growth factor receptor 2 regulates proliferation and Sertoli differentiation during male sex determination. *Proc Natl Acad Sci USA*. 2007;104:16558-16563.
17. Miyawaki S, Kuroki S, Maeda R, Okashita N, Koopman P, Tachibana M. The mouse Sry locus harbors a cryptic exon that is essential for male sex determination. *Science*. 2020;370:121-124.
18. Carlsson P, Waterman ML, Jones KA. The hLEF/TCF-1 alpha HMG protein contains a context-dependent transcriptional activation domain that induces the TCR alpha enhancer in T cells. *Genes Dev*. 1993;7:2418-2430.
19. Vainio S, Heikkila M, Kispert A, Chin N, McMahon AP. Female development in mammals is regulated by Wnt-4 signalling. *Nature*. 1999;397:405-409.
20. Jeays-Ward K, Dandonneau M, Swain A. Wnt4 is required for proper male as well as female sexual development. *Dev Biol*. 2004;276:431-440.
21. Rahmoun M, Lavery R, Laurent-Chaballier S, et al. In mammalian foetal testes, SOX9 regulates expression of its target genes by binding to genomic regions with conserved signatures. *Nucleic Acids Res*. 2017;45:7191-7211.
22. Belanger C, Berube-Simard FA, Leduc E, et al. Dysregulation of cotranscriptional alternative splicing underlies CHARGE syndrome. *Proc Natl Acad Sci U S A*. 2018;115:E620-E629.
23. Berube-Simard FA, Pilon N. Molecular dissection of CHARGE syndrome highlights the vulnerability of neural crest cells to problems with alternative splicing and other transcription-related processes. *Transcription*. 2019;10:21-28.
24. Kalantari R, Chiang CM, Corey DR. Regulation of mammalian transcription and splicing by Nuclear RNAi. *Nucleic Acids Res*. 2016;44:524-537.
25. Schnetz MP, Handoko L, Akhtar-Zaidi B, et al. CHD7 targets active gene enhancer elements to modulate ES cell-specific gene expression. *PLoS Genet*. 2010;6:e1001023.
26. Hurd EA, Capers PL, Blauwkamp MN, et al. Loss of Chd7 function in gene-trapped reporter mice is embryonic lethal and associated with severe defects in multiple developing tissues. *Mamm Genome*. 2007;18:94-104.
27. Mazaud Guittot S, Tetu A, Legault E, Pilon N, Silversides DW, Viger RS. The proximal Gata4 promoter directs reporter gene expression to sertoli cells during mouse gonadal development. *Biol Reprod*. 2007;76:85-95.
28. Pilon N, Raiwet D, Viger RS, Silversides DW. Novel pre- and post-gastrulation expression of Gata4 within cells of the inner cell mass and migratory neural crest cells. *Dev Dyn*. 2008;237:1133-1143.
29. Boulende Sab A, Bouchard MF, Beland M, et al. An Ebox element in the proximal Gata4 promoter is required for Gata4 expression in vivo. *PLoS One*. 2011;6:e29038.
30. Sanchez-Ferras O, Bernas G, Laberge-Perrault E, Pilon N. Induction and dorsal restriction of Paired-box 3 (Pax3) gene expression in the caudal neuroectoderm is mediated by integration of multiple pathways on a short neural crest enhancer. *Biochim Biophys Acta*. 2014;1839:546-558.

31. Soret R, Mennetrey M, Bergeron KF, et al. A collagen VI-dependent pathogenic mechanism for Hirschsprung's disease. *J Clin Invest*. 2015;125:4483-4496.

32. Cardinal T, Bergeron KF, Soret R, et al. Male-biased aganglionic megacolon in the TashT mouse model of Hirschsprung disease involves upregulation of p53 protein activity and Ddx3y gene expression. *PLoS Genet*. 2020;16:e1009008.

33. Wang J, Vasaikar S, Shi Z, Greer M, Zhang B. WebGestalt 2017: a more comprehensive, powerful, flexible and interactive gene set enrichment analysis toolkit. *Nucleic Acids Res*. 2017;45:W130-W137.

34. Pilon N, Daneau I, Paradis V, et al. Porcine SRY promoter is a target for steroidogenic factor 1. *Biol Reprod*. 2003;68:1098-1106.

35. Kasah S, Oddy C, Basson MA. Autism-linked CHD gene expression patterns during development predict multi-organ disease phenotypes. *J Anat*. 2018;233:755-769.

36. Viger RS, Mertineit C, Trasler JM, Nemer M. Transcription factor GATA-4 is expressed in a sexually dimorphic pattern during mouse gonadal development and is a potent activator of the Mullerian inhibiting substance promoter. *Development*. 1998;125:2665-2675.

37. Schmahl J, Eicher EM, Washburn LL, Capel B. Sry induces cell proliferation in the mouse gonad. *Development*. 2000;127:65-73.

38. Tevosian SG, Albrecht KH, Crispino JD, Fujiwara Y, Eicher EM, Orkin SH. Gonadal differentiation, sex determination and normal Sry expression in mice require direct interaction between transcription partners GATA4 and FOG2. *Development*. 2002;129:4627-4634.

39. Bajpai R, Chen DA, Rada-Iglesias A, et al. CHD7 cooperates with PBAF to control multipotent neural crest formation. *Nature*. 2010;463:958-962.

40. Batsukh T, Pieper L, Koszucka AM, et al. CHD8 interacts with CHD7, a protein which is mutated in CHARGE syndrome. *Hum Mol Genet*. 2010;19:2858-2866.

41. Batsukh T, Schulz Y, Wolf S, et al. Identification and characterization of FAM124B as a novel component of a CHD7 and CHD8 containing complex. *PLoS One*. 2012;7:e52640.

42. Feng W, Kawauchi D, Korkel-Qu H, et al. Chd7 is indispensable for mammalian brain development through activation of a neuronal differentiation programme. *Nat Commun*. 2017;8:14758.

43. Zentner GE, Hurd EA, Schnetz MP, et al. CHD7 functions in the nucleolus as a positive regulator of ribosomal RNA biogenesis. *Hum Mol Genet*. 2010;19:3491-3501.

44. Miyamoto Y, Taniguchi H, Hamel F, Silversides DW, Viger RS. A GATA4/WT1 cooperation regulates transcription of genes required for mammalian sex determination and differentiation. *BMC Mol Biol*. 2008;9:44.

45. Rappsilber J, Ryder U, Lamond AI, Mann M. Large-scale proteomic analysis of the human spliceosome. *Genome Res*. 2002;12:1231-1245.

46. Jameson SA, Natarajan A, Cool J, et al. Temporal transcriptional profiling of somatic and germ cells reveals biased lineage priming of sexual fate in the fetal mouse gonad. *PLoS Genet*. 2012;8:e1002575.

47. Young RM, Ewan KB, Ferrer VP, et al. Developmentally regulated Tcf7l2 splice variants mediate transcriptional repressor functions during eye formation. *Elife*. 2019;8:e51447.

48. Tanwar PS, Kaneko-Tarui T, Zhang L, Rani P, Taketo MM, Teixeira J. Constitutive WNT/beta-catenin signaling in murine Sertoli cells disrupts their differentiation and ability to support spermatogenesis. *Biol Reprod*. 2010;82:422-432.

49. Chen SR, Liu YX. Testis cord maintenance in mouse embryos: genes and signaling. *Biol Reprod*. 2016;94:42.

50. Cool J, DeFalco T, Capel B. Testis formation in the fetal mouse: dynamic and complex de novo tubulogenesis. *Wiley Interdiscip Rev Dev Biol*. 2012;1:847-859.

51. Chen SR, Chen M, Wang XN, et al. The Wilms tumor gene, Wt1, maintains testicular cord integrity by regulating the expression of Col4a1 and Col4a2. *Biol Reprod*. 2013;88:56.

52. Chen YS, Racca JD, Phillips NB, Weiss MA. Inherited human sex reversal due to impaired nucleocytoplasmic trafficking of SRY defines a male transcriptional threshold. *Proc Natl Acad Sci U S A*. 2013;110:E3567-3576.

53. Bergman JE, Bosman EA, van Ravenswaaij-Arts CM, Steel KP. Study of smell and reproductive organs in a mouse model for CHARGE syndrome. *Eur J Hum Genet*. 2010;18:171-177.

54. Pierucci-Alves F, Clark AM, Russell LD. A developmental study of the Desert hedgehog-null mouse testis. *Biol Reprod*. 2001;65:1392-1402.

55. Balasubramanian R, Crowley WF Jr. Reproductive endocrine phenotypes relating to CHD7 mutations in humans. *Am J Med Genet C Semin Med Genet*. 2017;175:507-515.

56. Anderzen-Carlsson A. CHARGE Syndrome-a five case study of the syndrome characteristics and health care consumption during the first year in life. *J Pediatr Nurs*. 2015;30:6-16.

57. Bergman JE, de Wijs I, Jongmans MC, Admiraal RJ, Hoefsloot LH, van Ravenswaaij-Arts CM. Exon copy number alterations of the CHD7 gene are not a major cause of CHARGE and CHARGE-like syndrome. *Eur J Med Genet*. 2008;51:417-425.

58. Husu E, Hove HD, Farholt S, et al. Phenotype in 18 Danish subjects with genetically verified CHARGE syndrome. *Clin Genet*. 2013;83:125-134.

59. Jongmans MC, Admiraal RJ, van der Donk KP, et al. CHARGE syndrome: the phenotypic spectrum of mutations in the CHD7 gene. *J Med Genet*. 2006;43:306-314.

60. Ragan DC, Casale AJ, Rink RC, Cain MP, Weaver DD. Genitourinary anomalies in the CHARGE association. *J Urol*. 1999;161:622-625.

61. Shoji Y, Ida S, Etani Y, et al. Endocrinological characteristics of 25 Japanese patients with CHARGE syndrome. *Clin Pediatr Endocrinol*. 2014;23:45-51.

62. Stromland K, Sjogreen L, Johansson M, et al. CHARGE association in Sweden: malformations and functional deficits. *Am J Med Genet A*. 2005;133A:331-339.

63. Tellier AL, Cormier-Daire V, Abadie V, et al. CHARGE syndrome: report of 47 cases and review. *Am J Med Genet*. 1998;76:402-409.

64. Vissers LE, van Ravenswaaij CM, Admiraal R, et al. Mutations in a new member of the chromodomain gene family cause CHARGE syndrome. *Nat Genet*. 2004;36:955-957.

SUPPORTING INFORMATION

Additional supporting information may be found in the online version of the article at the publisher's website.